10th ANKARA INTERNATIONAL AEROSPACE CONFERENCE AIAC-2019-036
18-20 September 2019 - METU, Ankara TURKEY

ION OPTICS SYSTEM ANALYSIS OF THE RF-ICP ION THRUSTER

Erdal Bozkurt[1] and Ümmügül Erözbek Güngör[2]
Middle East Technical University
Ankara, TURKEY

Nafiz Alemdaroğlu[3]
Atılım University
Ankara, TURKEY

ABSTRACT

This work presents the theoretical analysis of ion optics system (IOS) of the two-gridded RF-ICP ion thruster. The simulations of this system are done by using the COMSOL Multiphysics software program. Distributions of the electric potential and the field of the three-coil ion thruster in 2D space are examined. In addition, perveance and ion beam trajectory of the system are studied. For ion thrusters, the flow of the extracted beam and the shape of sheath edge can be categorized in three perveance cases. Among these three, the optimum is the most desired case for getting high performance. At constant voltage, there is a linear relationship between the perveance and the Child current. At constant Ar gas pressure, trust and Isp increase with the RF power. Similarly, they increase with the pressure at constant RF power. The ion beam trajectories are investigated for different particle number and different emitting origin. The particle numbers are selected as 20 and 100. Flat, concave and convex shape particle emitting origins are chosen. Ion beam trajectories become well focused (optimum-perveance) when they are released from the convex surface.

INTRODUCTION

In general, the ion optics (extraction) system is composed of three main parts, which are screen grid, accelerator grid and decelerator grid. However, in this study, two-grid geometry is used. In this geometry, there are two electrostatic stainless steel grids. These grids are placed a few mm apart to each other. The first grid that is very close to the plasma chamber is called as screen grid. The generated plasma ions are extracted from this grid toward to the second grid that is known as the accelerator grid. By applying negative voltage with respect to the potential of the screen grid, the second grid accelerates the ions with high velocities out of the thruster [Bumbarger, 2013]. The main functions of the ion optics system are controlling the ion current, increasing the ion beam quality, minimizing the ion losses and preventing the electrode corrosion.

[1] M.S. Student in Aerospace Engineering Department, METU, Email: e169695@metu.edu
[2] PhD in Physics Department, METU, Email: ummugul@metu.edu
[3] Prof, Civil Aviation High School, in Atılım University, Email: nafizalemdaroglu@atilim.edu.tr

Perveance

The perveance is defined as the extracted current from the accelerating grid for a specific voltage (space charge limit) and the grid geometry [Botha, 2014]. According to the Child Langmuir limit, it is very important to decide size of the screen grid gap distance (aperture) to get maximum perveance. Mathematical expression of the maximum normalized perveance per hole is given in following Equation 1 [Williams, 2013; Botha, 2014; Dobkevicius, 2017; Farnell, 2007; Brown, 2004];

$$P_{max} = \frac{\pi\varepsilon_0}{9}\sqrt{\frac{2q}{m_i}}\left(\frac{D_s}{l_e}\right)^2 \left[A/V^{3/2}\right] \quad (1)$$

where m_i is the mass of the used propellant gas, D_s is the aperture diameter of the screen grid and l_e is the effective sheath thickness. From the Equation1, there is an upper limit to the normalized perveance per hole for a particular propellant.

Basically, the perveance phenomenon is described under three subtitles; under perveance, optimum perveance and over perveance.

Under Perveance: When the extracted ion current is too low than the applied screen voltage, the shape of sheath edge becomes curved or the effective sheath thickness (l_e), which is shown in Figure 1-a, increases. This condition is known as under perveance [Williams, 2013; Brown, 2004]. As shown in the Figure 1-b, the ion beam is not well-focused when passing through the accelerator grid.

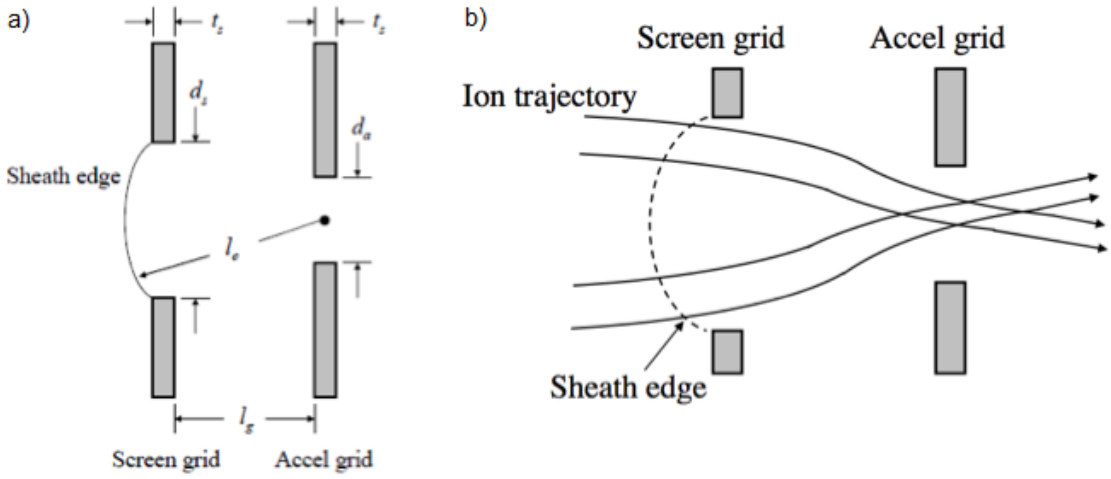

Figure 1: a) Dimensions of the grids b) Under-perveance [Williams, 2013]

Optimum Perveance: When the extracted ion beam is well focused and the shape of sheath edge a bit smoother than the under-perveance, this condition is called as optimum perveance [Williams, 2013]. In this case, the beam is not crossing; ion loss is minimum and no contact with the grids. The optimal case is the half of maximum perveance written in the Equation1 that can be obtained by changing the grid potentials [Williams, 2013; Brown, 2004].

Over Perveance: The case that the ion beam is much higher than the applied voltage and the curve is very smooth is defined as the over perveance as clearly seen in Figure 2. In this case, the plasma density is high whereas the electron temperature is low and the effective sheath thickness (l_e) decreases [Williams, 2013; Brown, 2004].

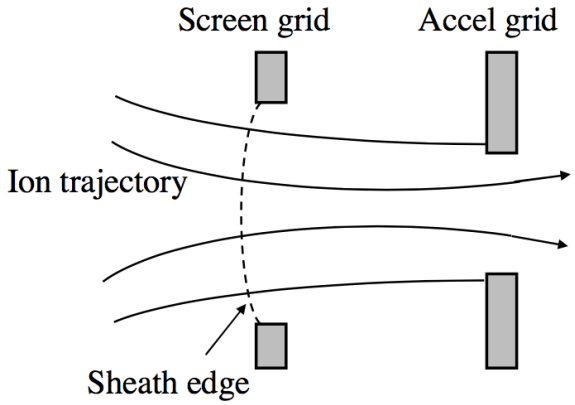

Figure 2: Over-perveance [Williams, 2013]

Ion Trajectories

The relation between the perveance and the ion trajectories is clearly seen in Figure 3. From under-perveance to optimum-perveance, the trajectories become well focused and no contact with the grids. Therefore, in this direction, the system is protected from the grid erosion. From optimum perveance to over perveance, the particles contact more with the grids and so grid lifetime decreases [Dobkevicius, 2017; Brown, 2004].

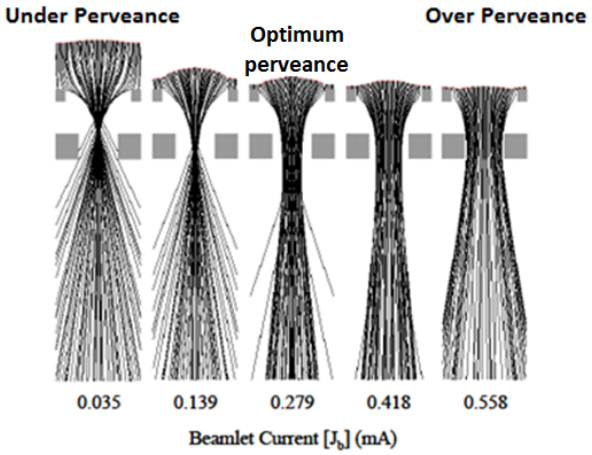

Figure 3: Ion trajectories according to the perveance [Farnell, 2007]

METHOD

The COMSOL Model

In this study, two modules of the COMSOL software program are used. These modules are electrostatic module and charged particle tracing module. By using the electrostatic module, we get strength and directions of the electrostatic field while ion trajectories are obtained by using the charged particle tracing module.

Electrostatic module: The electric field analysis is done according to the following two basic well-known relations.

$$\nabla . \vec{D} = \nabla . \left(\varepsilon_0 \varepsilon_r \vec{E} \right) = \rho_V \quad (2)$$

$$\vec{E} = -\nabla V \tag{3}$$

where ε_0 is the permitivity of the air, ε_r is the relative permittivity, ρ_V is the volume charge density, E is the E-field and V is the electric potential.

Therefore, the E-field in any direction can be solved by negative rate of change of the electric potential and also E-field can be obtained from the charge conservation.

The selected conditions for this module are; V_{anode} is 100 V, V_{screen} is 70 V, V_{acc} is -352 V and V_{space} is -195.4 V.

Charged particle tracing module: Ion trajectories can be drawn by solving following force equations.

$$\overrightarrow{F_e} = \frac{d(m_p \vec{v})}{dt} \quad \text{where} \quad m_p = \frac{m_r}{\sqrt{1 - v.v/c^2}} \tag{4}$$

$$\overrightarrow{F_e} = ez\vec{E} \tag{5}$$

where m_r is the particle (Ar) rest mass, e is the unit charge (C), F_e is the electrical force, v is the ion velocity and c is the speed of light.

The selected conditions for this module are; Z (charge number) is 1, N (particle number per release) is 100, v_{0y} (initial particle velocity in the y-direction or Bohm velocity at the sheath edge) is approximately 3000 m/s.

RESULTS AND DISCUSSION

The simulated set-up is composed of two main parts; plasma chamber and ion optics system as shown in Figure 4. Three-turn coil is wrapped around the plasma chamber. Two-grid ion optics system is placed on the chamber. The green electrode is the screen grid while the magenta electrode is accelerator grid. There are eighty-five grid holes on the each grid.

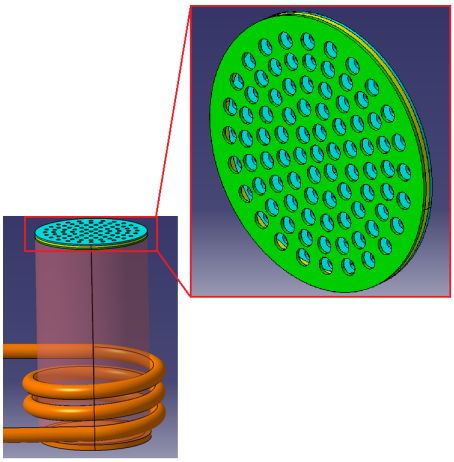

Figure 4: The simulated plasma chamber and ion optics system

In order to study the electric potential and the electric field variations in 2D space, the simulations are initiated at the COMSOL electrostatic module without using ions extraction. Therefore, first of all, 2D ion optics solution domain is created as shown in Figure 5.

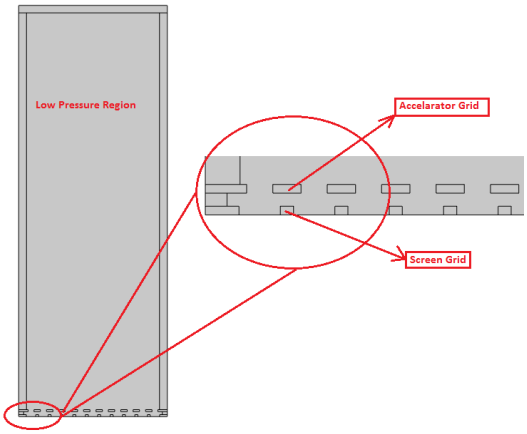

Figure 5: Simulation geometry of the RF-ICP ion thruster

Potential and electric field variations along this solution domain are shown in Figure 6. From the Figure 6-a, maximum positive potential onto the screen grids is 70 V and maximum negative potential onto the accelerator grids is - 352 V. At the boundary of the domain, the space potential is -195,4 V.

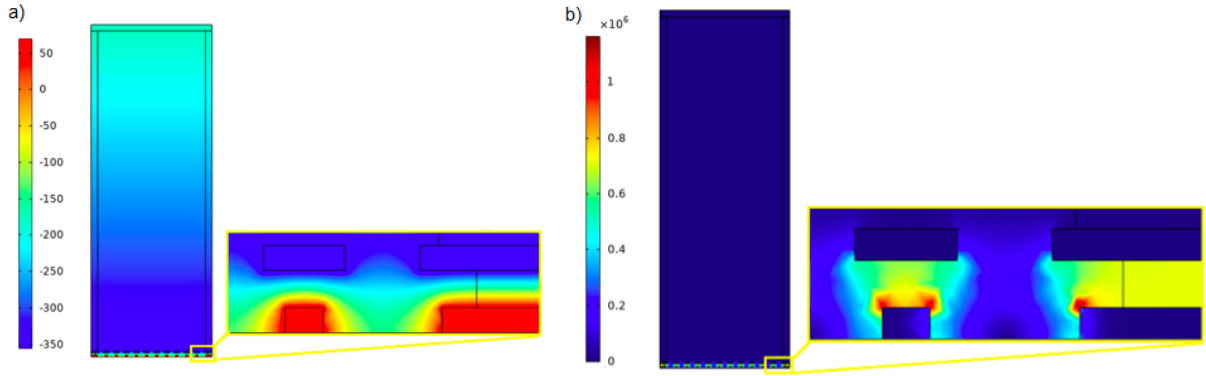

Figure 6: a) Potential (Volts) and b) the magnitude of the electric field distributions (Volts/m) throughout the whole simulated domain

In Figure 6-b, the magnitude of the electric field distribution along the domain is clearly seen. At the sharp edges, the field strength has the highest value. As we know, the electric field is zero in the metals (grids). Between the grids, the field strength is also high enough. It decreases while getting further away.

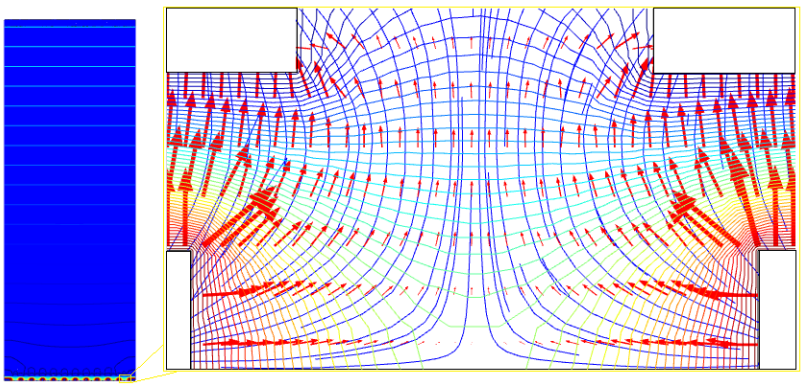

Figure 7: The electric potential (Volts) iso-counter distribution (colored lines) and the streamlines (red arrow) of the electric fields (Volts/m) throughout the whole simulated domain

As seen in Figure 7, The E-field streamlines are perpendicular to the electric potential lines. Also, the E-field lines penetrate to the metal surface as known from the electro-magnetism.

Perveance

Voltage and current dependencies of the perveance are shown in Figure 8. In Figure 8-a, there is an inverse relation between the perveance and voltage at constant pressure and Child current. On the other hand, from the Figure8-b, the perveance increases with the Child current at constant voltage. For this system, the perveance is P=2.189x10^{-6} A/V$^{3/2}$, when the Child limited current is I=18,98 mA.

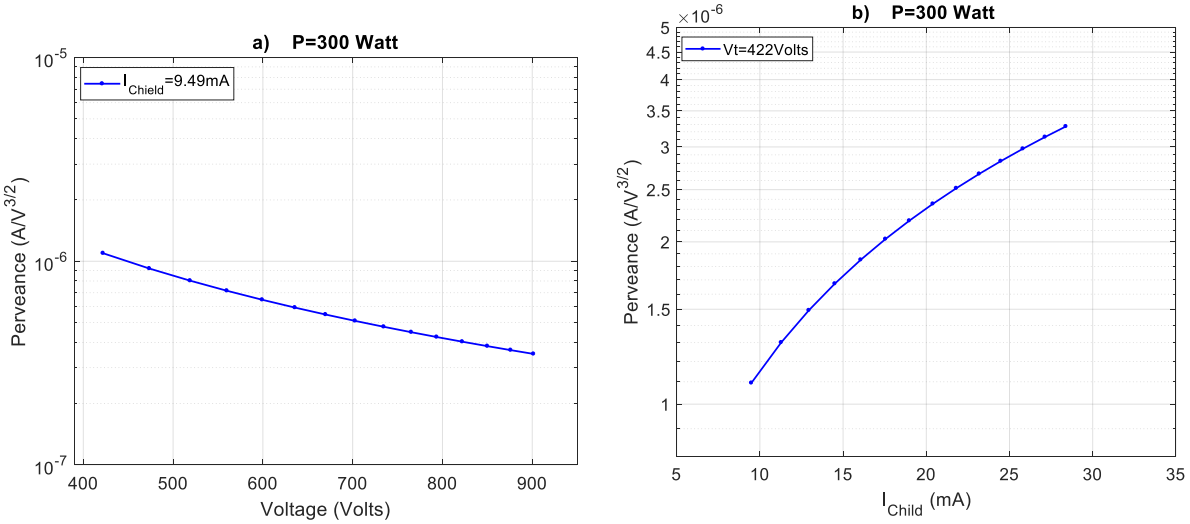

Figure 8: Perveance analysis with respect to a) voltage and b) maximum Child current

New Approach for Trust and Isp

In this section, trust and Isp calculations were done according to the maximum perveance. There is a close relationship between the perveance and the effective sheath thickness that is given in Equation 1. Also, the relation between the effective thickness and the other dimensional parameters is shown in following Equation 6 [Turkoz, 2014; Farnell, 2007].

$$l_e = \sqrt{\left(l_g + t_s\right)^2 + \frac{D_s^2}{4}} \tag{6}$$

where l_e is the effective length (sheath thickness), l_g is the distance between screen and accelerator grids (hot grid gap), t_s is the thickness of the grids and D_s is diameter of the screen grid.

The dimensions of the simulated ion optics geometry; D_s is 1.9 mm, t_s is 0.4 mm, l_g is 0.6 mm and l_e is 1.4 mm.

For Argon gas and 85 grids, the perveance is found as 1.095×10^{-6} A.V$^{-3/2}$

When we set the RF power to 300 Watt, the ion density (n_i) is 5.13×10^{16} m^{-3} and the electron temperature (T_e) is 3.43625 eV at the sheath edge.

The COMSOL ion current is 5.7 mA (total area-2.41×10^{-4} m^2 and ion flux-23.63 A.m^{-2}). When the accepted ion extraction capacity is 60%, the Child ion current becomes 9.5 mA. Now, we can calculate the potential between the grids (V_T) from Equation 7.

$$V_T = \left(\frac{I_{Child}}{P_{max}}\right)^{2/3} \tag{7}$$

From the Equation 7, V_T is 422 Volt. When we take the voltage ratio of net acceleration voltage (V_N) per V_T as 0.7, V_N becomes 295.4 Volt.

Then, the trust can be calculated from Equation 8 [Farnell, 2007].

$$T = I_{Comsol}\sqrt{\frac{2M_i V_N}{e}} \tag{8}$$

By using the Equation 8, the trust is found as 0.0891 mN.

Also, Isp is calculated as 3848 sec from Equation 9 [Farnell, 2007].

$$Isp = \frac{1}{g}\sqrt{\frac{2eV_N}{M_i}} \tag{9}$$

where g is 9.81 m.s^{-2}.

Evolutions of the Trust and Isp with respect to the RF power at constant pressure are shown in Figure 9. Trust gradually increases with the RF power from 0.01 to 1.1 mN. This results match with that of some other research [Dobkevicius, 2017; Lotz, 2013; Tsuan-Tsay, 2006]. Also, a decreasing increase is seen in the value of the Isp with the power from 2000 to 6000 sec [Tsuan-Tsay, 2006].

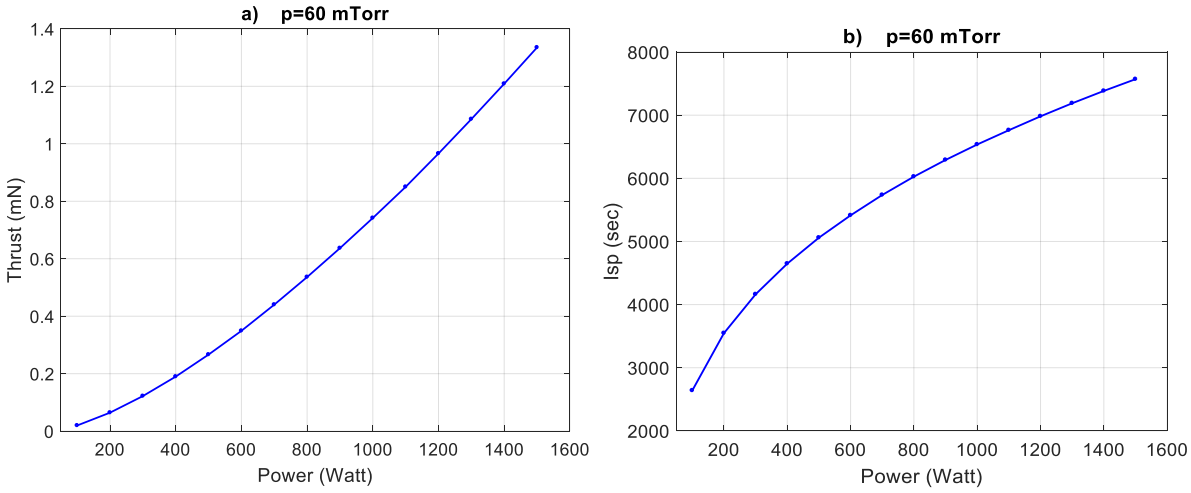

Figure 9: a) Trust and b) Isp variations with respect to RF power

Pressure dependencies of the Trust and Isp at constant RF power are clearly seen in Figure 10. Thrust linearly increases with the pressure from 0.09 to 0.41 mN whereas a descending increase is observed in the value of Isp with the gas pressure from 3800 to 5600 sec.

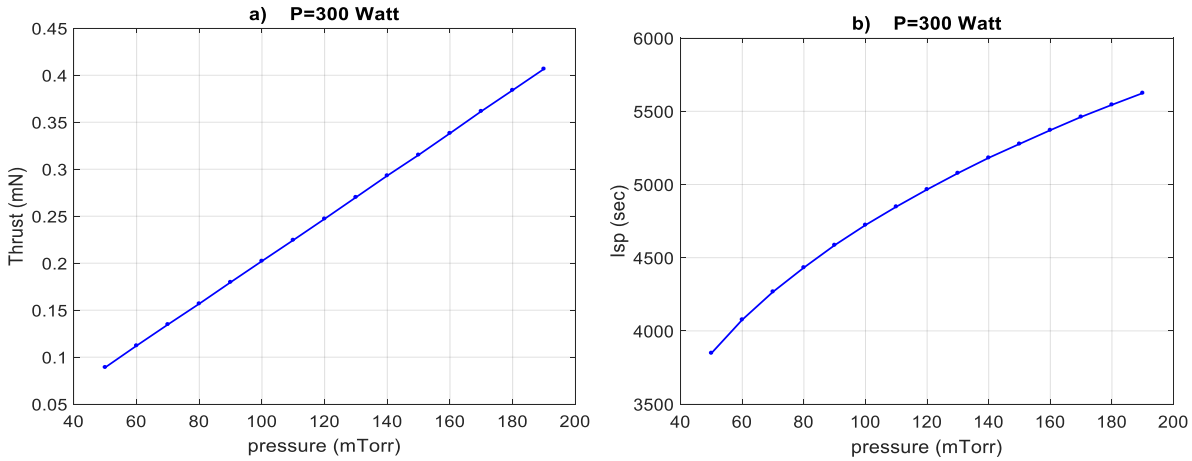

Figure 10: a) Trust and b) Isp variations with respect to Ar gas pressure

Ion Trajectories

Figures 11-13 show the ion trajectories and equipotential lines of the ion optics system under different source origin. In the Figure 11, the sheath assumed to be flat and the ions released from this flat line by changing the particle number. As compared both shapes, the trajectories are completely the same like a cone. This condition is called as under-perveance.

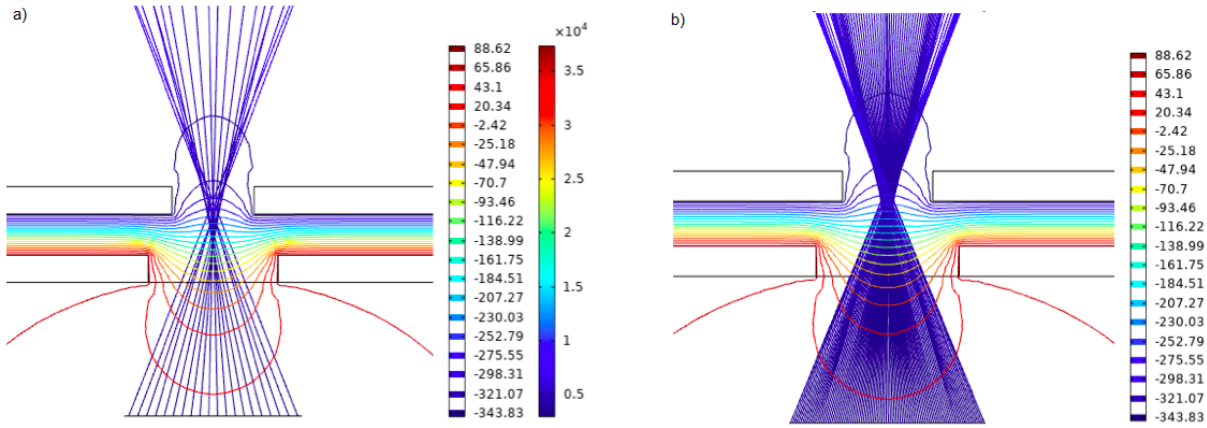

Figure 11: Blue lines in the y-axis depict ion trajectories of a) N=20 b) N=100 ions that are released from the flat line and the other colored lines depict the equipotential lines

When the origin of the particles is changed to a concave surface, the particles are scattered more. Again, the crossing trajectories are seen. Therefore, the condition is under-perveance.

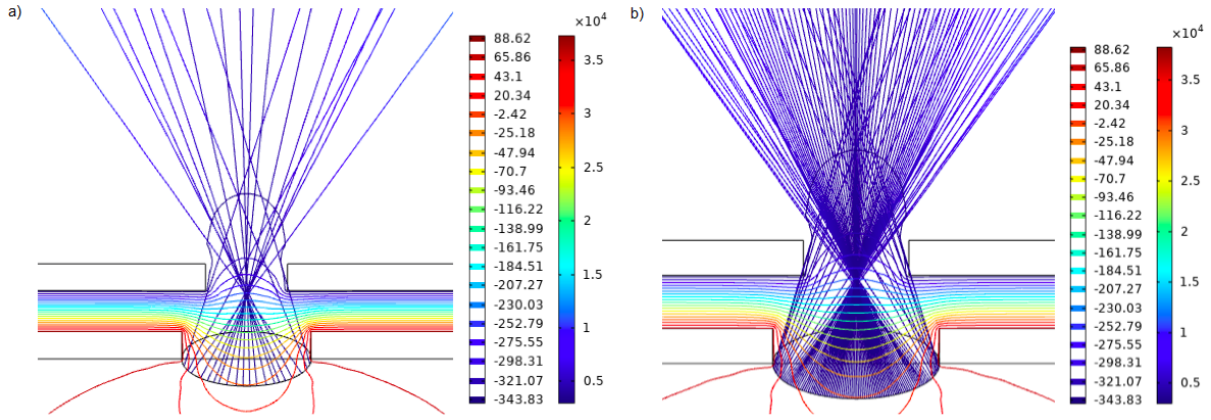

Figure 12: Blue lines in the y-axis depict ion trajectories of a) N=20 b) N=100 ions that are released from the specified concave surface and the other colored lines depict the equipotential lines

From the Figure 13, well-focused ion beam is clearly observed with the 100 number particles that are released from the convex surface. Almost none particle strikes to the grids. This condition is the optimum-perveance condition. As compared to the other conditions, the beamlet current is the highest at this time.

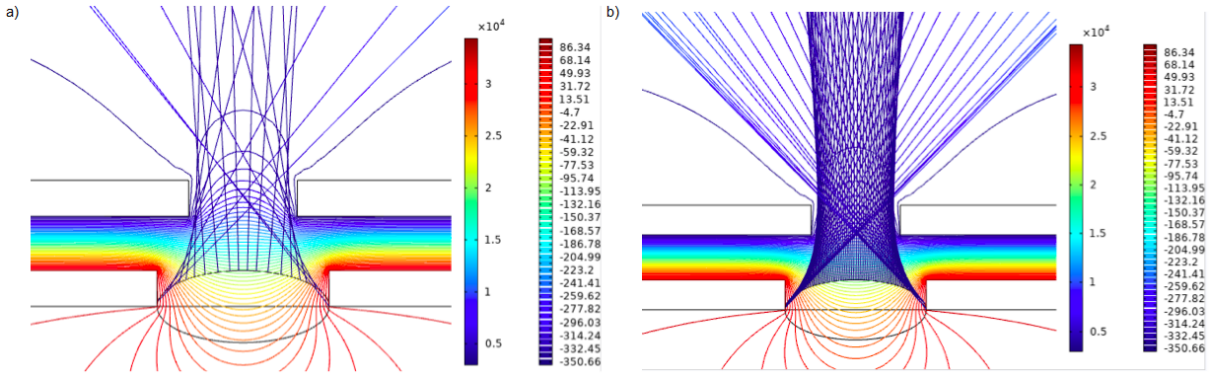

Figure 13: Blue lines in the y-axis depict ion trajectories of a) N=20 b) N=100 ions that are released from the specified convex surface and the other colored lines depict the equipotential lines

In conclusion, the ion optics system of an RF-ICP ion thruster is investigated in this paper.

Electrostatics and charged particle tracing modules of the COMSOL program are run together. Perveance property of the system is analyzied. For the fixed current, the perveance decreases with the applied voltage. On the other hand, for the fixed voltage, a decreasing increase in the value of perveance is seen with the current. Finally, when the particle releasing origin is a flat line, the condition is under-perveance as written in literature. On the other hand, the perveance condition is optimum while the origin is convex and this result is different from the knowledge mentioned in some papers [Farnell, 2007]. In other words, for constant particle number, if the plasma meniscus shape changes from planar to convex, the perveance is also changed from under to optimum [Brown, 2004]. Trust and Isp are calculated from the maximum normalized perveance. These results are more compatible with the other research results.

References

Brown, I. G. (2004) *The Physics and Technology of Ion Sources*, Second Edition, Wiley VCH, 2004.

Bumbarger, P. P. (2013) *Analysis of a Miniature Radio Frequency Ion Thruster with an Inductively Coupled Plasma Source*, M.S. Thesis, Boise State University, December 2013.

Botha, J. R. (2014) *Design of an RF Ion Thruster*, M.S. Thesis, Stellenbosch University, April 2014.

Dobkevicius, M. (2017) *Modeling and Design of Inductively Coupled Radio Frequency Gridded Ion Thrusters with an Application to Ion Beam Shepherd Type Space Missions,* PhD Thesis, University of Southampton, June 2017.

Farnell, C. C. (2007) *Performance and Lifetime Simulation of Ion Thruster Optics,* PhD Thesis, Colorado State University, Spring 2007.

Lotz, B. (2013) *Plasma physical and material physical aspects of the application of atmospheric gases as a propellant for Ion-Thruster of the RIT-Type***,** PhD Thesis, Giessen University, May 2013.

Turkoz, E., Sik F. and Celik M. (2014) *A Study of Ion Thruster Optics through Particle Simulations and Evaluation of the Near Plume Plasma Properties*, American Institute of Aeronautics and Astronautics, August 2014.

Tsuan-Tsay, M. M. (2006) *Numerical Modeling of a Radio-Frequency Micro Ion Thruster*, Ms Thesis, MIT, May 2006.

Williams, L.T. (2013) *Ion Acceleration Mechanisms of Helicon Thrusters*, PhD Thesis, Georgia Institute of Technology, May 2013.